ELSEVIER

Journal of Hazardous Materials 140 (2007) 200–204

Journal of Hazardous Materials

www.elsevier.com/locate/jhazmat

Photocatalytic degradation of gaseous benzene over TiO_2/Sr_2CeO_4: Preparation and photocatalytic behavior of TiO_2/Sr_2CeO_4

Junbo Zhong, Jianli Wang, Lin Tao, Maochu Gong, Liu Zhimin, Yaoqiang Chen *

College of Chemistry, Sichuan University, Sichuan 610064, PR China

Received 29 April 2006; received in revised form 1 June 2006; accepted 19 June 2006
Available online 29 June 2006

Abstract

The paper demonstrates that the photocatalytic activity of TiO_2 towards the decomposition of gaseous benzene in a batch reactor can be greatly improved by loading TiO_2 on the surface of Sr_2CeO_4. The research investigates the optimum loading amount of TiO_2 on Sr_2CeO_4 in enhancing the photocatalytic activity of TiO_2. The prepared photocatalyst was characterized by XRD, UV–vis diffuse reflectance and XPS analyses. TiO_2 is loaded on Sr_2CeO_4 at 773 K. TiO_2/Sr_2CeO_4 absorbs much more visible light than TiO_2. The XPS spectrum shows that there are Ti, O, C, Sr elements on the surface of the TiO_2/Sr_2CeO_4, and that the binding energy value of Ti2p transfers to a lower value. TiO_2/Sr_2CeO_4 demonstrates 2.0 times the photocatalytic activity of pure TiO_2. Based upon these observations, the mechanistic role of Sr_2CeO_4 in the photocatalytic oxidation reaction has been suggested.

Keywords: Photocatalysis; TiO_2; Sr_2CeO_4; Benzene; Photocatalytic oxidation

1. Introduction

Volatile organic compounds (VOCs), especially aromatic hydrocarbons, are typical pollutants emitted from numerous urban and industrial sources. Many of the VOCs in common use are toxic and some are considered to be carcinogenic, mutagenic, or teratogenic [1]. Among the technologies developed for the treatment of VOCs, the photocatalytic oxidation process is considered to be a promising technology. Photocatalytic oxidations have an advantage over other technologies, such as thermal incineration and catalytic incineration, in that they can efficiently decompose low concentrations of VOCs under mild conditions [2]. It is likely that this air purification technology offers strong advantages, but deactivation of the titanium dioxide catalyst during gas–solid photocatalytic oxidation of air contaminated by VOCs is a serious issue and deserves attention from industrial application and academic researchers [3].

Zhang et al. [4] investigated the gas-phase photocatalytic reaction of benzene in a recirculation photocatalytic system. Their results showed that the concentration of benzene clearly decreased when the initial concentration was less than 100 mg/m^3, with no change detected after 140 min when the initial concentration up to 300 mg/m^3, there is hence no photocatalytic activity for higher concentration of benzene. Sauer et al. [5] noted catalyst deactivation for a toluene and perchloroethylene feed mixture in air. Pierre and David [6] treated TiO_2 with water and HCl, and noticed that when the concentration of benzene was 50 mg/m^3, benzene conversion over TiO_2/H_2O reached 80% and dropped slowly to 30% in about 3 h because of deactivation of photocatalyst. The benzene conversion over TiO_2/HCl remained nearly constant at about 25% for the entire 6 h run due to its low photocatalytic activity.

The decomposition of volatile organic compounds has been difficult because of the low conversion and the common deactivation of photocatalyst. Therefore, it is crucial to prolong the lifetime of the photocatalyst and enhance its photocatalytic activity. Various techniques have been developed for development and modification of the TiO_2-based photocatalysts [7].

Sr_2CeO_4 is blue-white phosphor, it can exhibit photoluminescence under excitation with irradiation of ultraviolet rays [8]. The excitation spectra present two broad bands with maxima at 280 and 340 nm and the emission spectrum has a broad band centered at 465 nm [9]. To our knowledge, there are few reports on the photocatalytic activity of TiO_2 loaded on Sr_2CeO_4.

* Corresponding author. Tel.: +86 28 85418451.
E-mail addresses: scuzhong@sina.com (J. Zhong), liuzhimin2648@sina.com (L. Zhimin), zhongjunbo@sohu.com (Y. Chen).

0304-3894/$ – see front matter © 2006 Elsevier B.V. All rights reserved.
doi:10.1016/j.jhazmat.2006.06.063

Nomenclature

C_0	Initial concentration of gaseous benzene ($mg\,L^{-1}$)
C	Concentration of gaseous benzene at monent ($mg\,L^{-1}$)
ΔE_b	The binding energy difference, $\Delta E_b = E_b(Ti2p_{1/2}) - E_b(Ti2p_{3/2})$
RH	Relative humidity (%)
t	Reaction time (min)

Benzene is a major indoor and industrial air pollutant, and it was recommended as one of the eight representative indoor VOCs. In the present paper, benzene was therefore chosen as the model VOC to investigate the capability with TiO_2/Sr_2CeO_4. The objective of this work is to prolong the lifetime of the photocatalyst and enhance its photocatalytic activity by loading TiO_2 onto the fluorescent material Sr_2CeO_4. This paper presents the experimental results and proposes the role of Sr_2CeO_4 in the photocatalytic oxidation reaction.

2. Experimental

2.1. Preparation of TiO_2/Sr_2CeO_4

All reagents, which were analytic, were purchased from Chendu Kelong chemical reagents factory and used as received. Deionized water was used throughout the experiments.

2.9526 g $SrCO_3$ and 1.7212 g CeO_2 were mixed and finely ground in agate mortar for 1 h, then fired at 1273 K in ceramic crucible for 4 h in air. Finally, the Sr_2CeO_4 superfine particles were obtained.

Precursor solution for TiO_2 was prepared by the following method. Tetrabutylorthotitanate (17.2 mL) and diethanolamine (4.8 mL) were dissolved in ethanol (67.28 mL). After stirring vigorously for 2 h at room temperature, a mixed solution of water (0.9 mL) and ethanol (10 mL) was added dropwise to the above solution under stirring. The resultant alkoxide solution was kept standing at room temperature for hydrolysis during 2 h, resulting in the TiO_2 sol. The composition ratio of $Ti(OC_4H_9)_4$, C_2H_5OH, H_2O and $NH(C_2H_4OH)_2$ in the starting alkoxide solution was 1:26.5:1:1 (in molar ratio). The pure TiO_2 powder was prepared after calcination the TiO_2 gel at 773 K.

The photocatalyst of TiO_2/Sr_2CeO_4 with different loaded amounts of TiO_2 (wt%) was prepared by impregnating method using TiO_2 sol, then cacinated at 773 K for 2 h.

2.2. Charaterization of TiO_2/Sr_2CeO_4

Surface area analysis of TiO_2/Sr_2CeO_4 was carried out by the Brunauer-Emmet teller (BET) method using Autosorb-ZXF-05 (Xibei Chemical Institute, China). X-ray diffraction patterns were recorded with a DX-1000 X-ray diffraction (XRD) using Cu Kα radiation, 40 kV, 20 mA. XPS measurement was carried out on a spectrometer (XSAM-800, KRATOS Co.) with Mg Kα anticathode. The UV–vis diffuse reflectance spectrum was performed on a spectrometer (TU-1907). Changes in the amount of TiO_2 loading were determined in terms of the Ti^{4+}–H_2O_2 by the colorimetric spectrophotometer at 410 nm.

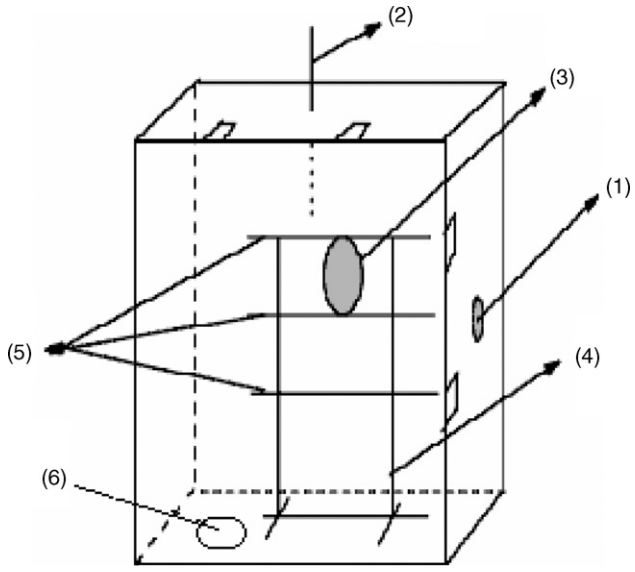

Fig. 1. Schematic diagram of the batch photocatalytic reactor: (1) sampling point; (2) thermometer; (3) electric fan; (4) bracket; (5) germicidal lamp; (6) hygrometer.

2.3. Evaluation of the photocatalysis

Experiments were carried out in a closed stainless steel reactor with the volume of 105 L. An electric fan and three 10 W germicidal lamps with maximum wavelength of 253.7 nm were installed on a bracket (see Fig. 1). Twenty grams of photocatalyst powder was dispersed in a thin layer over two aluminum foils with the total area of 980 cm^2, and the required quantity of liquid benzene was injected into the reactor. Once dark-adsorption equilibrium has been reached, photocatalysis is started by turning on the UV light source. The initial concentration of benzene was kept at 1000 mg/m^3 for all the experiments. The photocatalytic oxidation of benzene was performed under illumination at 312–313 K to avoid condensation of benzene by placing two infrared lamps outside the reactor. The concentration of benzene was detected by gas-phase chromatogram with FID detector and GDX-101 chromapack column. The gas was withdrawn regularly from the reactor for analysis.

In this paper, the conversion rate was calculated by $(C_0 - C)/C_0$, where C is the concentration of the reactant after irradiation as a function of reaction time and C_0 is the concentration of the reactant after adsorption equilibrium and before the irradiation in the presence of catalyst.

3. Results and discussion

3.1. Blank experiments

The reference experiments were carried out in two conditions: one with illumination but no catalyst, the other with TiO_2 (pure

Table 1
Relationship between benzene conversion and TiO_2 loading of TiO_2/Sr_2CeO_4 after reaction for 2 h (RH: 50%)

TiO_2 loading (%)	Surface area ($m^2\ g^{-1}$)	Conversion rate (%)
0.5	14.72	35.25
1.0	20.08	50.00
1.5	14.67	45.32
2.0	13.83	40.29
4.0	8.89	38.92

TiO_2 and TiO_2/Sr_2CeO_4) but no illumination. The results show that the concentration of benzene (1000 mg/m^3) changes so little under these conditions that conversion can be ignored. The blank tests proved the stability of benzene rings. Without illumination or photocatalyst, benzene is thermodynamically stable. It is also suggested that dark adsorption for benzene from gas-phase is small; therefore, the adsorption equilibrium can be established quickly.

3.2. Photocatalytic activity at different TiO_2 loading

In heterogeneous photocatalysis, the photocatalytic activity of catalyst not only depends on properties of loading species, but also on the amount of compound loaded. We investigated the photoactivity of different TiO_2 loadings on Sr_2CeO_4. Table 1 shows that the conversion rate of benzene increases and then drops as the TiO_2 loading increases. The highest efficiency of 50% is obtained when the TiO_2 loading is 1.0%, then the photodegradation efficiency drops sharply at 4.0%. It is suggested that a low content of TiO_2 cannot provide enough TiO_2 photocatalyst, while a large amount of TiO_2 may lead to a drop in the conversion of benzene due to the nucleation of TiO_2 on the support, which decreases the amount of TiO_2 surface. The data of surface area of different TiO_2 loading is consistent with the photocatalytic activity of different TiO_2 loadings on Sr_2CeO_4. We therefore selected 1.0% of TiO_2 loading on Sr_2CeO_4.

3.3. Characterization of the catalyst

The XRD patterns of 1.0 wt% TiO_2/Sr_2CeO_4 is shown in Fig. 1. Pure titania exhibits stronger anatase diffraction peaks of (1 0 1), (0 0 4), (2 0 0) and (2 1 1) at 25.2°, 37.8°, 48.04° and 55.02°, respectively, indicating that TiO_2/Sr_2CeO_4 is anatase and no rutile is found. All diffraction peaks of B in Fig. 2 can be assigned to the single-phase Sr_2CeO_4 with the orthorhombic structure. This observation is consistent with the data reported by Tang et al. [10,11], indicating that pure Sr_2CeO_4 is obtained at 1273 K for 4 h,no presence of CeO_2, $SrCO_3$, $SrCeO_3$ are revealed by XRD patterns of 1.0 wt% TiO_2/Sr_2CeO_4. The reaction steps leading to the formation of Sr_2CeO_4 can be proposed as follows [12]:

$$SrCO_3 + CeO_2 \rightarrow SrCeO_3 + CO_2$$

$$SrCeO_3 + SrCO_3 \rightarrow Sr_2CeO_4 + CO_2$$

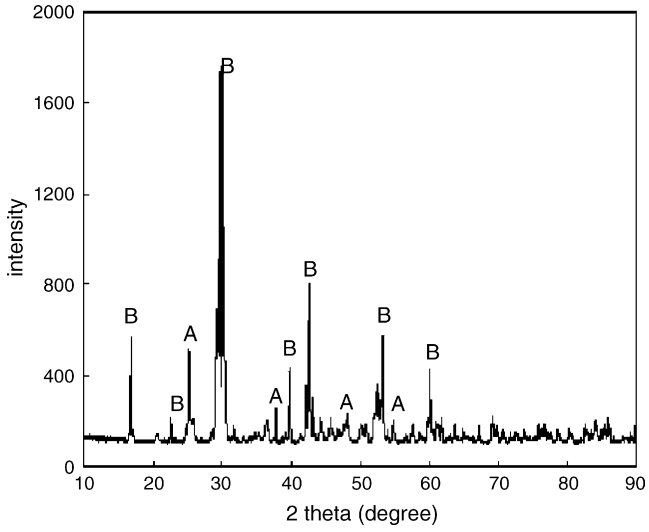

Fig. 2. The XRD patterns of the catalyst: (A) anatase of TiO_2; (B) Sr_2CeO_4.

Since the pure and loaded titania samples were prepared for use in the photocatalytic reaction, their UV–vis diffuse reflective properties may have had a strong effect on the photocatalytic activity. Fig. 3 shows the diffuse reflectance spectrum of pure and loaded TiO_2.

As shown in Fig. 2, from 210 to 300 nm, two spectra have an obvious difference, TiO_2/Sr_2CeO_4 reflects much more ultraviolet light than TiO_2, which indicates that TiO_2 absorbs much more ultraviolet light than TiO_2/Sr_2CeO_4. It is plausible that Sr_2CeO_4 reflects a portion of ultraviolet light. From 300 to 400 nm, there is no difference between the two spectra. However, the presence of Sr_2CeO_4 clearly changes the spectra of TiO_2 in the visible light regions, TiO_2/Sr_2CeO_4 absorbs much more visible light than TiO_2. The results show that TiO_2/Sr_2CeO_4 can be excited by visible light.

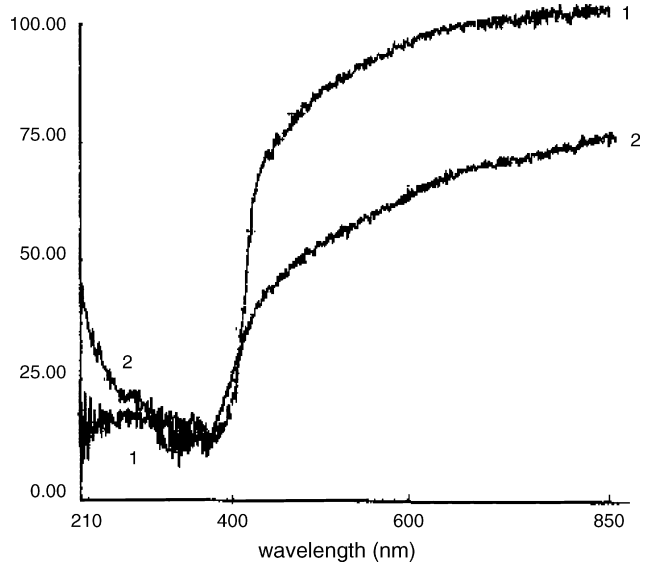

Fig. 3. UV–vis diffuse reflectance spectra: (1) TiO_2; (2) TiO_2/Sr_2CeO_4 (1.0 wt%).

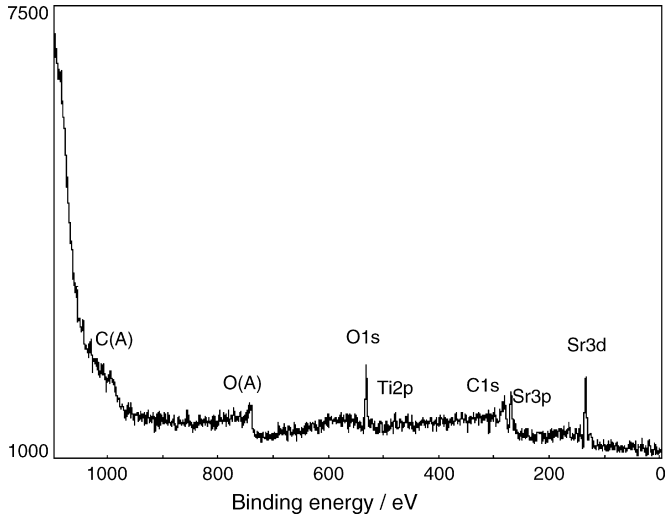

Fig. 4. XPS survey spectrum for the surface of TiO_2/Sr_2CeO_4.

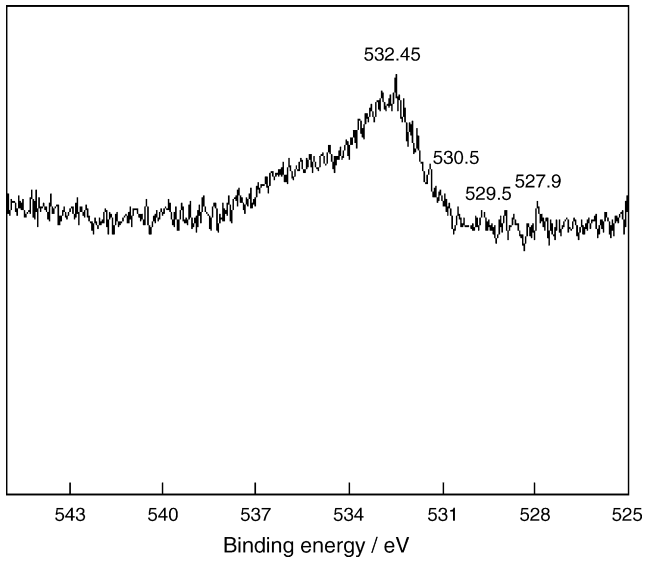

Fig. 5. O (1s) XPS spectrum.

The XPS spectrum (Fig. 4) shows that there are Ti, O, C, Sr elements on the surface of the TiO_2/Sr_2CeO_4. The Ti element resulted from the precursor solution. The O element is assigned to the precursor solution and Sr_2CeO_4. The Sr element resulted from Sr_2CeO_4. The C element probably came from the organic radicals of precursor for the sol–gel method, which were not completely burnt out during heat-treatment. No Ce element was detected on the surface of the TiO_2/Sr_2CeO_4.

The high resolution XPS spectrum corresponding to the surface of TiO_2 was characterized by a main doublet composed of two symmetric peaks situated at $E_b(Ti2p_{3/2}) = 458.9$ eV and $E_b(Ti2p_{1/2}) = 464.6$ eV (Table 2), the binding energy difference, $\Delta E_b = E_b(Ti2p_{1/2}) - E_b(Ti2p_{3/2})$ was 5.7 eV, as previously reported in the literature [13], but as for TiO_2/Sr_2CeO_4, only $E_b(Ti2p_{3/2}) = 458.2$ eV was detected, no $E_b(Ti2p_{1/2})$ was observed. Compared with pure TiO_2, the $E_b(Ti2p_{3/2})$ of TiO_2/Sr_2CeO_4 is transferred to a lower value, the result indicates that Ti forms strong radical links through oxygen bridges with Sr_2CeO_4. So, it is obvious that there is stronger interaction between Sr_2CeO_4 and TiO_2.

Further information of the surface can be also obtained from the O (1s) XPS spectrum. The O (1s) peaks of TiO_2/Sr_2CeO_4 are presented in Fig. 5. The peak at 532.45 eV is assigned to the lattice oxygen of Sr_2CeO_4 crystal (O^{2-}) and the lower binding energy 527.9 eV corresponded to O^{2-} ion at the bridging site on the topmost layer of the Sr_2CeO_4 surface. The peak at 529.5 eV is assigned to O (1s) (TiO_2), the peak at 530.5 eV corresponded to O (1s) (C–O).

Table 2
Peak fitting results of the high-resolution spectra of the Ti2p

Sample	Ti2p		
	$E_b(Ti2p_{1/2})$	$E_b(Ti2p_{3/2})$	ΔE_b
TiO_2	464.6	458.9	5.7
TiO_2/Sr_2CeO_4	–	458.2	–

3.4. Comparison the photoactivity of TiO_2/Sr_2CeO_4 and TiO_2

The photocatalytic activity of TiO_2/Sr_2CeO_4 and TiO_2 are compared and presented in Fig. 6.

As shown in Fig. 6, in the process of decomposing, the pure TiO_2 deactivates after 2 h, and the maximum conversion of 32.0% is reached after 2 h, while the 1.0 wt% loaded catalyst exhibits its superiority stability. In the whole process of reaction, the conversion rate keeps increasing until 4 h when the photocatalytic activity begins to decline and the maximum conversion of 65.0% is reached. Moreover, the conversion rate is 2.0 times that of the pure TiO_2. It is seen that the TiO_2 loaded on Sr_2CeO_4 can prolong the life of photocatalyst and enhance the photocatalytic activity of catalyst.

3.5. Proposed mechanism

The photocatalytic activity of TiO_2 is not high enough to be useful for industrial purpose [14]. Several methods have been

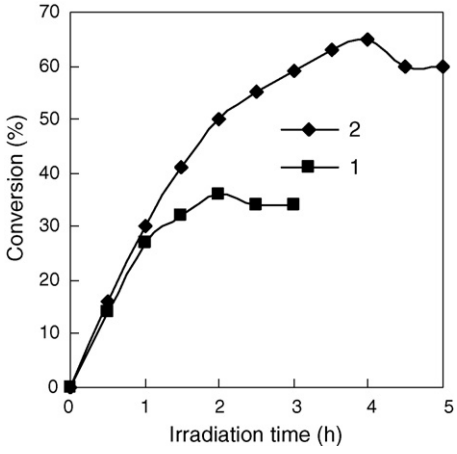

Fig. 6. Conversion of benzene vs. irradiation time: (1) TiO_2; (2) TiO_2/Sr_2CeO_4 RH: 50%.

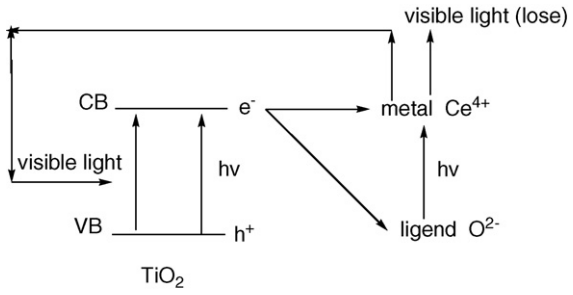

Fig. 7. Scheme depicting electron transfer of TiO_2/Sr_2CeO_4.

attempted to improve the photocatalytic efficiency, such as pressing the recombination of electron–hole pairs and enhancing of visible light response [15]. In this paper, TiO_2/Sr_2CeO_4 exhibits stronger photocatalytic activity than pure TiO_2. It is plausible that the stronger photocatalytic activity of TiO_2/Sr_2CeO_4 results from two factors.

The first factor is that the presence of Sr_2CeO_4 can prolong the life of electron–hole pairs and reduce the recombination of electron–hole pairs. The Sr_2CeO_4 compound possesses one-dimensional chain of edge-sharing CeO_6 octahedra, in which the cerium ion is in the 4+ (IV) state and its 4f shell is empty. The blue luminescence from Sr_2CeO_4 was suggested from a ligand O^{2-}-to-metal Ce^{4+} charge transfer [8]. Considering that an electron can be transferred from an oxygen ligand to the empty 4f shell of Ce^{4+}, a high spin triplet excited state is formed via a spin forbidden transfer. Therefore, the photoluminescence of Sr_2CeO_4 can be assigned to a ligand O^{2-}-to-metal Ce^{4+} transfer transition of Ce^{4+} [8,10]. In the present paper, Sr_2CeO_4 was used as support, TiO_2 was loaded on the surface of Sr_2CeO_4, when TiO_2 absorbs photons (recall the light with the maximum wavelength of 253.7 nm), electrons are excited from the valence to the conduction band leaving holes behind. When Sr_2CeO_4 absorbs ultraviolet ray, ligand O^{2-}-to-metal Ce^{4+} charge transfer forms, it will emit blue light; if the excited electron of TiO_2 transfer to ligand O^{2-} or metal Ce^{4+}, thus the recombination of electron–hole pairs can be pressed, which result in promotion of the photocatalytic activity of TiO_2. The electron transfer mechanism is shown in Fig. 7.

The second factor is TiO_2/Sr_2CeO_4 increases the absorption in the region 400–850 nm. The emission spectrum of Sr_2CeO_4 has a broad band centered at 465 nm [10], part of the light emitted by Sr_2CeO_4 can excite TiO_2, thus the photocatalytic activity can be promoted.

From the above discussion, it is clear that the two factors have a synergy which increases the photocatalytic activity of TiO_2/Sr_2CeO_4.

4. Conclusions

The paper revealed that the optimal loading amount of TiO_2 on Sr_2CeO_4 in our experimental condition for the degradation of gaseous benzene was 1 wt%. The characterization results of XRD indicate that TiO_2 loaded on Sr_2CeO_4 is anatase at 773 K firing temperature. TiO_2/Sr_2CeO_4 absorbs much more visible light than TiO_2. The XPS spectrum shows that there are Ti, O, C, Sr elements on the surface of the TiO_2/Sr_2CeO_4, and that the binding energy value of Ti2p transfers to a lower value. In the process of decomposing benzene, the pure TiO_2 deactivates after 2 h, and the maximum conversion of 32.0% is reached after 2 h. The conversion rate on TiO_2/Sr_2CeO_4 keeps increasing until 4 h when the photocatalytic activity begins to decline and the maximum conversion of 65.0% is reached. The proposed mechanism is synergy of electron transfer and the stronger absorption in the region 400–850 nm.

References

[1] W. Wen, C.L. Wei, K. Young, Decomposition of benzene in air streams by UV/TiO_2 process, J. Hazard. Mater. B 101 (2003) 133–146.
[2] E. Hisahiro, F. Shigeru, I. Takashi, Heterogeneous photocatalytic oxidation of benzene, toluene, cyclohexene and cyclohexane in humidified air: comparison of decomposition behavior on photoirradiated TiO_2 catalyst, Appl. Catal. B: Environ. 38 (2002) 215–225.
[3] M.M. Ameen, G.B. Raupp, Reversible catalyst deactivation in the photocatalytic oxidation of dilute *o*-xylene in air, J. Catal. 184 (1999) 112–122.
[4] Q.C. Zhang, F.Y. Zhang, G.L. Zhang, X.P. Zhang, Gas-phase photo catalytic reaction properties of benzene on TiO_2, Chin. Environ. Sci. 23 (2003) 661–664.
[5] M.L. Sauer, M.A. Hale, D.F. Ollis, Heterogeneous photocatalytic oxidation of dilute toluene-chlorocarbon mixtures in air, J. Photochem. Photobiol. A: Chem. 88 (1995) 169–178.
[6] O.H. Pierre, P.F. David, Benzene and toluene gas-phase photocatalytic degradation over H_2O and HCL pretreated TiO_2: by-products and mechanisms, J. Photochem. Photobiol. A: Chem. 118 (1998) 197–204.
[7] T.K. Kim, M.N. Lee, S.H. Lee, Y.C. Park, C.K. Jung, J.H. Boo, Development of surface coating technology of TiO_2 powder and improvement of photocatalytic activity by surface modification, Thin Solid Films 475 (2005) 171–177.
[8] M. Toshiyuki, C. Takanobu, I. Nobuhito, G.Y. Adachi, Synthesis and luminescence of Sr_2CeO_4 fine particles, Mater. Res. Bull. 38 (2003) 17–24.
[9] S.L. Fu, J. Dai, F.F. Zhou, Synthesis of Sr_2CeO_4 phosphorby mechanical and reactive sintering, Chin. J. Inorg. Chem. 20 (2004) 698–702.
[10] Y.X. Tang, H.P. Guo, Q.Z. Qin, Photoluminescence of Sr_2CeO_4 phosphors prepared by microwave calcination and pulsed laser deposition, Solid State Commun. 121 (2002) 351–356.
[11] S.J. Chen, X.T. Chen, Z. Yu, J.M. Hong, Z.L. Xue, X.Z. You, Preparation and characterization of fine Sr_2CeO_4 blue phosphor powders, Solid State Commun. 130 (2004) 281–285.
[12] Y.B. Khollam, S.B. Deshpande, P.K. Khanna, P.A. Joy, H.S. Potdar, Microwave-accelerated hydrothermal synthesis of blue-white phosphor: Sr_2CeO_4, Mater. Lett. 58 (2004) 2521–2524.
[13] J.G. Yu, X.J. Zhao, Q.N. Zhao, J.C. Du, XPS of study of TiO_2 photocatalytic thin film prepared by the sol–gel method, Chin. J. Mater. Res. 14 (2000) 203–209.
[14] T.K. Young, Y.S. Kang, I.L. Wan, J.C. Guang, R.D. Young, Photocatalytic behavior of WO_3-Loaded TiO_2 in an oxidation reaction, J. Catal. 191 (2000) 192–199.
[15] P. Bonamali, S. Maheshwar, N. Gyoichi, Preparation and characterization of TiO_2/Fe_2O_3 binary mixed oxides and its photocatalytic properties, Mater. Chem. Phys. 59 (1999) 254–261.